

# Photon Bound States in Coupled Waveguides

Björn Schrinski,<sup>1</sup> Johan A. Brimer,<sup>1</sup> and Anders S. Sørensen<sup>1</sup>

<sup>1</sup>*Center for Hybrid Quantum Networks (Hy-Q), The Niels Bohr Institute, University of Copenhagen, Blegdamsvej 17, 2100 Copenhagen, Denmark*

Photon bound states have been identified as particular solutions to the scattering of two photons from a single emitter, but from these results the full nature of these states remains elusive. We study a novel, clear and unambiguous signature that these bound states are truly bound. To this end we consider a new configuration of close-by waveguides, each chirally coupled to two-level emitters. We show that in this system the photon bound states behave like rigid molecules, where photons do not tunnel individually but rather collectively, such that there is rarely a single photon in each waveguide. We further identify new classes of bound states in this system.

*Introduction*–Photons hardly interact directly, but can interact indirectly through coupling to matter [1]. In systems with photons coupled to quantum emitters it makes intuitive sense that effects like the exclusion of multiple excitations of the same emitter combined with stimulated emission lead to strong correlations in the emitted photons. These correlations can reach the degree that photons are “bound” to each other [2–5], interact attractively or repulsively [6–8], scatter inelastically [9, 10] and may even form some kind of quasi matter. In this way, setups consisting of waveguides coupled to two- or multi-level emitters [11] can be used to create a range of interesting phenomena, e.g. from new quantum many-body states of light [10, 12–20] to non-linear phase shifts enabling quantum computation schemes [21–24].

Here we consider bound states of photons. Such “photonic-molecules” are the quantum limit of optical solitons [25–27]. They have been predicted in a range of systems such as two- [2, 3, 6, 7, 28, 29] and three-level systems [8] coupled to waveguides as well as atomic gases with Rydberg interaction [30–32]. Experimentally, bound states have been observed in Rydberg atomic ensembles [5] and with a quantum dot coupled to an optical cavity [33]. The dispersion relation of the bound states can be related to particles possessing mass, but such analogies raise the question of whether this is just a mathematical analogy or if the bound photons also act in a collective manner when being manipulated, i.e. do they behave as “truly distinct physical objects” [27]?

We want to continue this train of thought by considering the very basic question, do photons in a bound state stick together when we try to separate them? To answer this, we consider a scenario where we allow photons to tunnel between two nearby waveguides, each chirally coupled to two-level emitters that decay by emitting photons [34, 35] into the waveguide with a decay rate  $\Gamma$ . Such chiral systems, where emitters only emit photons in a single direction have been experimentally realized in Refs. [34–38]. For a single waveguide, this configuration is known to allow for the creation of photon bound states [8, 27]. We extend the model to two coupled waveguides to investigate what happens to the bound states when the photons can tunnel between the waveguides and thereby break apart the bound state. Co-

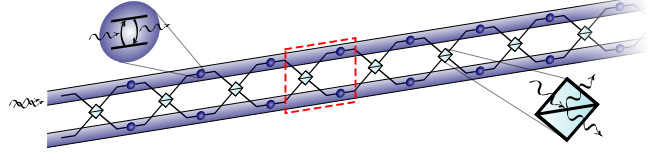


Figure 1. The considered setup consists of two one-dimensional photonic waveguides each chirally coupled to two-level quantum emitters. The waveguides are close enough to allow tunneling of photons from one to the other, which is modelled as beamsplitters with a high reflection probability. The red rhomb marks the unit cell used to describe the propagation.

herent tunneling is described by inserting a beamsplitter transformation after each emitter with a very large reflection probability  $P \simeq 1 - \theta^2$  where  $\theta \ll 1$ , see Fig. 1. In the linear scenario, i.e. without photon interactions, the individual photons would independently switch from one waveguide to the other and back again. For truly bound photons this slow continuous tunnelling should occur in pairs and should be suppressed as the probability to tunnel scales as  $(1 - P)^2 \simeq \theta^4$  since the photons have to switch waveguides simultaneously. In this paper we show that this is indeed the case, how new classes of bound states emerge in the setup, and that the different classes of bound and free photons can be distinguished by their deviating group velocities.

*Bound states*–The description of non-linear scattering of photons coupled to a single two-level system in general, and the emerging bound states in particular, was pioneered by Yudson [28] and finalized by Shen and Fan [2, 3] showing that the two photon Hilbert space can be divided into “free” and “bound” subspaces, described by the eigenstates  $|W_{k_1, k_2}\rangle$  and  $|B_K\rangle$ , respectively, where  $K = k_1 + k_2$  is the total energy (for simplicity we set group velocity and  $\hbar$  equal to unity such that decay rates and wavenumbers have the same dimensions). The bound states have the characteristic feature of being localized in position space [3], with the wavefunction

$$\langle x_1, x_2 | B_K \rangle = \frac{\sqrt{\Gamma}}{\sqrt{4\pi}} e^{iKX - \Gamma|\Delta|/2}, \quad (1)$$

being exponentially suppressed with the relative distance

coordinate  $\Delta = x_1 - x_2$  for two photons at locations  $x_1$  and  $x_2$  with center of mass coordinate  $X = (x_1 + x_2)/2$ . Here  $\Gamma$  denotes the decay rate of the emitter into the waveguide and we assume for simplicity that there are no other decay channels. On the other hand the unbound states are described by [3]

$$\langle x_1, x_2 | W_{k_1, k_2} \rangle = \frac{1}{\sqrt{2\pi^2}} e^{iKX} \times [2q \cos(q\Delta) - \Gamma \text{sgn}(x) \sin(q\Delta)], \quad (2)$$

where  $q = (k_1 - k_2)/2$  is the relative momentum.

The scattering process of a single emitter can be expressed in the complete basis of bound and unbound states via the (non-linear) scattering matrix [3]

$$S = \sum_{k_1 \leq k_2} t_{k_1} t_{k_2} |W_{k_1, k_2}\rangle \langle W_{k_1, k_2}| + \sum_K T_K |B_K\rangle \langle B_K|, \quad (3)$$

where

$$t_k = \frac{k - i\Gamma/2}{k + i\Gamma/2}, \quad \text{and} \quad T_K = \frac{K - 2i\Gamma}{K + 2i\Gamma} \quad (4)$$

are the linear phase shift acquired for an individual photon and the non-linear phase shift of the bound state, respectively. For chiral systems this dynamics can be extended to multiple emitters by repeated application of the scattering matrix. Such an extension to more emitters and photons opens up rich physics [27, 39–43] with e.g. bound states containing larger numbers of photons with associated increasing group velocities. The resulting spatial separation upon propagation allows for separating the different bound states and for example to study scattering with other photon states [27].

*Mathematical description*– We wish to describe a system where photons are distributed in two neighbouring waveguides denoted by  $a$  and  $b$ . In the momentum basis, states containing two photons can be written as

$$|\psi\rangle = \sum_{m, n \in a, b} \int dK dq \psi_{mn}(K, q) |K, q\rangle_{mn} \quad (5)$$

with basis states

$$|K, q\rangle_{mn} = c_m^\dagger(K/2 - q) c_n^\dagger(K/2 + q) |\text{vac}\rangle, \quad (6)$$

where  $c_a^\dagger(k)$  or  $c_b^\dagger(k)$  create a photon with momentum  $k$  in the upper or lower mode, respectively. We want to describe the system depicted in Fig.1 by merging the non-linear scattering and the tunneling transformation into one combined transformation  $T$  for each unit cell as defined by the red rhomb. We can project the different combinations of the two photons in the two waveguides into a vector  $\mathbf{v} = |\psi_{aa}, \psi_{ab}, \psi_{ba}, \psi_{bb}\rangle$  with  $|\psi_{mn}\rangle = \int dK dq |K, q\rangle_{mn} \langle K, q|_{mn} |\psi\rangle$ . For bosonic exchange symmetry reasons the second and third entry of

$\mathbf{v}$  are always equal. In this vector notation each unit cell transformation takes on the form

$$T = \text{diag}(S, S_{\text{lin}}, S_{\text{lin}}, S)(M \otimes M), \quad (7)$$

with the unitary tunneling matrix

$$M = \begin{pmatrix} \cos(\theta) & i \sin(\theta) \\ i \sin(\theta) & \cos(\theta) \end{pmatrix} \quad (8)$$

and the linear scattering matrix

$$S_{\text{lin}} = \sum_{m, n \in a, b} \sum_{K, q} t_{K/2 - q} t_{K/2 + q} |K, q\rangle_{mn} \langle K, q|_{mn}. \quad (9)$$

Here, the linear scattering describes the evolution of photons in separate waveguides, where there is no non-linear interaction between the photons. The state after  $N$  scattering events then reads  $T^N \mathbf{v}$ .

*Dynamics of bound states in coupled waveguides*– We now investigate various scenarios of photons scattering for the two waveguide setup. We consider a Gaussian product state of two photons entering the upper waveguide, i.e.  $\psi_{mn}(K, q) \propto \delta_{ma} \delta_{na} e^{-(k_1^2 + k_2^2)/2\sigma_k^2}$ , with  $\sigma_k = \Gamma/3$  to maximize the amplitude of the bound state [27]. The center of mass marginal population of photons after the last (here 70th) emitter are shown in Fig. 2 after Fourier transforming to position space and tracing over the relative coordinate  $\Delta$ . As a reference we first consider a single waveguide in Fig. 2 a). As discussed in detail in Ref. [27] there is a stark contrast between the non-linear and linear cases, where we replace  $S$  by  $S_{\text{lin}}$ . The combination of saturation of the emitters and stimulated emission between the photons leads to a faster group velocity for the bound state. As a consequence, when considering the Wigner delay, i.e. the delay relative to a non-interacting pulse, the linear case results in a slow, strongly dispersed state delayed by  $4N/\Gamma$  whereas the bound state traverses the setup much faster with a delay  $N/\Gamma$ .

Allowing for tunneling with a finite  $\theta$  in the linear setup, the population completely shifts from mode  $a$  to  $b$  after  $\pi/2\theta$  scattering events as shown in Fig. 2 b). After an integer times  $\pi/\theta$  scatterings, the population is back in the original waveguide, c.f. Fig. 2 c). In contrast, for the non-linear case we expect the emerging bound state to remain in the same waveguide for  $\theta \ll 1$ . This is confirmed in Fig. 2 b) where we observe that the bound state population remains almost unaffected by the tunneling, whereas the unbound population has tunnelled to the other waveguide.

To further investigate the tunnelling dynamics we divide the outgoing population into bound and unbound states based on their delay as indicated by the rectangle in Fig. 2 b). In Fig. 3 a) and b), we then consider how the population is distributed on the two waveguides inside and outside this window when we vary the number of scatterings. The window is defined such that all population is inside the window at  $N = 0$  (translating to  $X \in [-6.0, 6.0]$ ) and grows linearly with  $N$

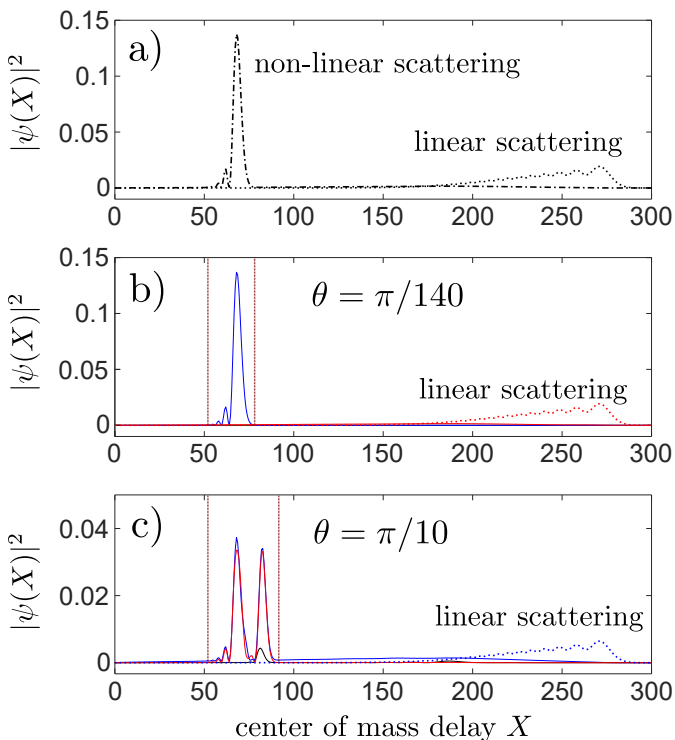


Figure 2. Center of mass distribution after  $N = 70$  scatterings. a) For a single waveguide in the linear regime (dotted curve) photons on resonance move the slowest with Wigner delay  $4N/\Gamma$  and strong dispersion due to the frequency width of the input state. Turning on the non-linearity (dashed dotted line) produces a bound state with group delay  $N/\Gamma$  and much less dispersion. b) A small tunneling probability ( $\theta = \pi/140$ ) between the two waveguides only allows unbound photons to switch to the  $bb$  mode (red curve) whereas the bound state remains practically in its entirety in the  $aa$  mode (blue curve). The mode with one photon in each path  $ab$  (black curve, hardly visible) is unoccupied. c) Increasing the tunneling amplitude ( $\theta = \pi/10$ ) shows the emergence of two classes of bound states with different group velocities, colors as in b).

to reach the size indicated in Fig. 2 b) (translating to  $X \in [53.3, 80.0]$ ). For small  $N$  the bound and unbound populations overlap and the population inside the window is unity in Fig. 3 a). As the bound and unbound populations separate, the population inside the window reaches a population around  $\sim 78\%$ , which is the bound state population for the chosen input state with  $\sigma_k = \Gamma/3$ . Furthermore, for the bound state both photons remain in the initial waveguide and do not separate. However, in case of the unbound contributions, Fig. 3 b), the photons tunnel independently and go to the other waveguide via an intermediate state with one photon in each waveguide. This behavior confirms the compound molecule-like behaviour of the photon bound state.

An even more convincing demonstration of the inseparable nature of bound photons would be if the bound

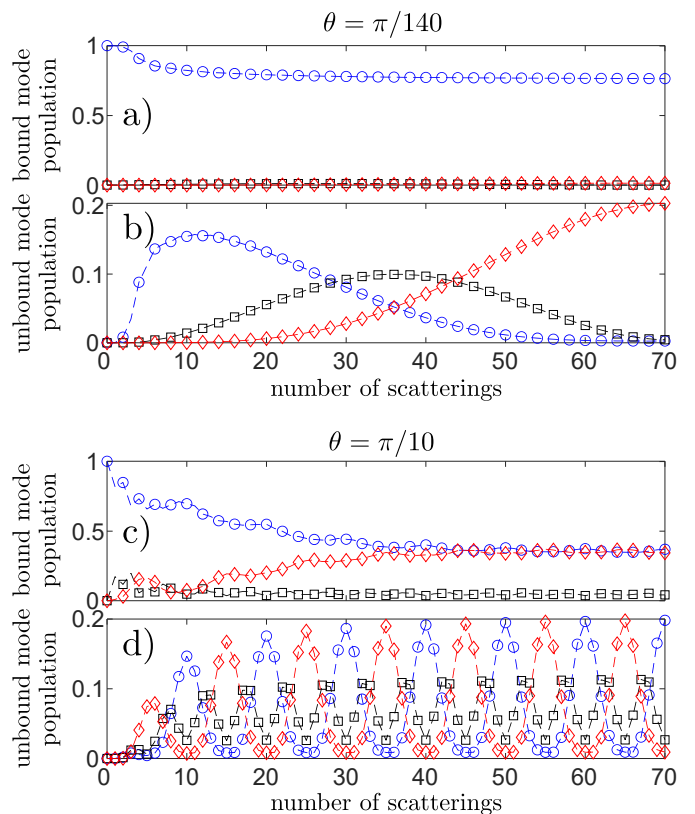


Figure 3. Populations of bound and unbound photons in the  $aa$  mode (blue circles),  $ab$  mode (black squares), and  $bb$  mode (red diamonds) after each scattering for two different tunnel probabilities,  $\theta = \pi/140$  (a,b) and  $\theta = \pi/10$  (c,d). To distinguish the bound (a,c) and unbound (b,d) populations we cut out windows around the bound states in the center of mass marginals, see Fig. 2. Since we observe almost no dispersion and a group delay  $\propto N$  [27] we scale the boundaries of the windows with  $N$ . Outside the windows the photons oscillate individually between the two waveguides with intermediate population of the  $ab$  mode. Inside the window the bound photons only jump in pairs. The bound state windows include a residue of unbound photons, leading to small oscillations in the bound state populations. In (a,b,c) we have removed every second point for better readability. The dashed lines are guides to the eye.

photons collectively switch modes. To show this, we increase the tunneling probability to  $\theta = \pi/10$  in Fig. 3 c) and d) so that free photons individually switch back and forth between the modes seven times after traversing  $N = 70$  emitters. The bound state instead slowly tunnels directly from mode  $aa$  to  $bb$  until an equilibrium is reached where it is equally likely to find the bound state in one or the other mode. Importantly, we again only find a small probability for the bound photons to be in two different waveguides. Here we chose the windows to be  $X \in [-6.0, 6.0]$  at  $N = 0$  shifting again linearly to  $X \in [53.3, 90, 6]$  at  $N = 70$  as shown in Fig. 2 c).

Due to the rather appreciable tunnelling  $\theta = \pi/10$ , the spatial distribution differs significantly from the case

without tunnelling. We now observe two distinct bound states of T, which travel at different group velocities, as shown in Fig. 2 c). The first is the anti-symmetric superposition of bound states in each waveguide  $|B_K\rangle_{aa} - |B_K\rangle_{bb}$ . Since this state is antisymmetric under the exchange of  $a$  and  $b$  it does not couple to  $ab$  components by tunnelling and it is an exact eigenstate for all  $\theta$ . Furthermore it has the same eigenvalue as the single waveguide bound state and thus travels at the same group velocity. The symmetric superposition  $|B_K\rangle_{aa} + |B_K\rangle_{bb}$ , however, is only an eigenstate if  $\theta = 0$ . For finite  $\theta$  it will couple to components with photons in different modes and as seen in Fig. 2 c) this slightly decreases the group velocity as photons in separate waveguides behave as free photons and thus move slower. We will explore these new bound states next.

*Stability of bound states*– To study these new classes of bound states in isolation, we chose as input state a Gaussian product state in a (anti)symmetric superposition  $\psi_{mn}(K, q) \propto \delta_{mn} e^{-(k_1^2 + k_2^2)/2\sigma_k^2}$  with a possible sign difference for the  $bb$  component. In Fig. 4 we depict the spatial wavefunction  $\Psi(X, \Delta)$  zooming in on the locations of the different bound states. All bound states show the typical exponential decay in the relative coordinate  $\Delta$ . The overall shapes of symmetric and anti-symmetric bound states are still close for small  $\theta = \pi/10$ , but there are larger deviations for  $\theta = \pi/4$  where we have the maximum amplitude for tunneling into the  $ab$  state. In this scenario the Hong-Ou-Mandel effect results in perfect switching between one photon in each waveguide ( $ab$ ) and a symmetric superposition of both photons in the same waveguide ( $aa$  and  $bb$ ) after every single scattering event. At  $\theta = \pi/4$  the symmetric bound state is the slowest with a delay time of  $2/\Gamma$  per emitter since it has the largest population in the  $ab$  mode where the photons do not increase the speed of each other by blocking emitters.

While the anti-symmetric state  $|B_K\rangle_{aa} - |B_K\rangle_{bb}$  is always a stable eigenstate state of the evolution due to symmetry, we have to resort to approximations to tackle the symmetric bound state for arbitrary  $\theta$ . For  $K = 0$  we observe that  $S|B_{K=0}\rangle = -|B_{K=0}\rangle$ , while  $S_{\text{lin}}|B_{K=0}\rangle = |B_{K=0}\rangle$  since  $t_k t_{-k} = 1$ . This allows us to find a *stable* eigenstate of the unit cell transformation (7) given by

$$|B_{K=0}\rangle_+ \propto |B_{K=0}\rangle_{aa} + i \tan(\theta) |B_{K=0}\rangle_{ab} + |B_{K=0}\rangle_{bb}, \quad (10)$$

showing that for small tunneling probabilities the population in the  $ab$  state is negligible  $\propto \theta^2$ .

For  $K \neq 0$  the  $ab$  component picks up  $k_1, k_2$  dependent phases relative to the  $aa$  and  $bb$  modes and we have not been able to identify exact eigenstates. We thus do not know if the state are true bound states or just metastable [6, 7, 43]. In the simulations, however, we have a finite momentum width and thus probe the behavior around  $K \approx 0$ . The tunneling amplitude  $\theta$  mainly affects the dispersion relation and we do not see strong differences

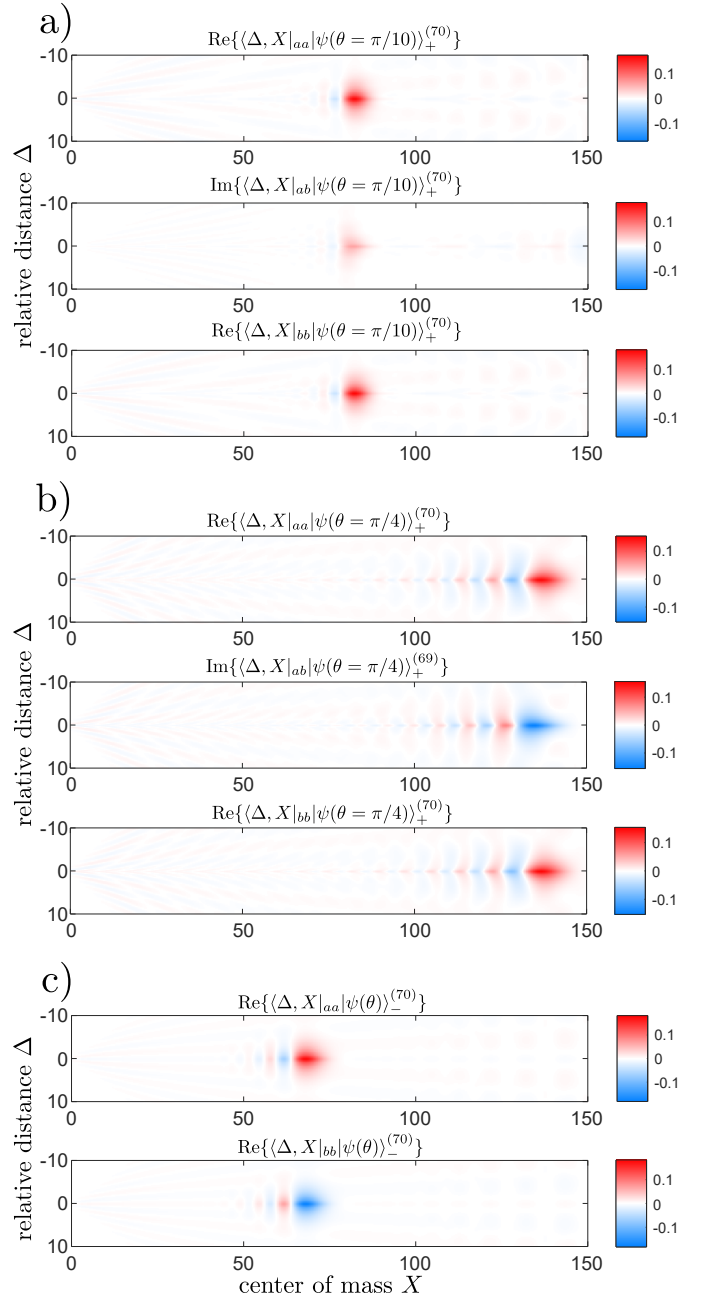


Figure 4. Real (or imaginary) part of the spatial wave functions with both photons in the upper ( $aa$ ), lower ( $bb$ ), or one in each path ( $ab$ ). The respective output state  $|\psi(\theta)\rangle_{\pm}^{(N)}$  after  $N$  scatterings is achieved with either a symmetric (+) or anti-symmetric (-) input Gaussian product state (see main text). a) For finite tunneling amplitudes  $\theta = \pi/10$  the symmetric bound state attains a small contribution in the  $ab$  mode. c) For  $\theta = \pi/4$ , the Hong-Ou-Mandel effect lets the bound state flip after every scattering between both photons being in the same path and both photons being in different paths. Note that the central plot is for  $N = 69$  and the top and lower plots are for  $N = 70$ . b) For reference, the anti-symmetric bound state is a stable eigenstate for all  $\theta$ . In all scenarios leaking from the bound states emerges as a faint leaking pattern over almost all phase space because the bound and unbound contribution cannot be distinguished exactly for finite number of scatterings.

between the bound state populations for the strongest tunneling  $\theta = \pi/4$  and  $\theta \rightarrow 0$  (Fig. 4 a and b) where  $|B_K\rangle_{aa} + |B_K\rangle_{bb}$  is an exact eigenstate. This suggests that the symmetric state is a stable eigenstate for  $K \approx 0$ . To test this we consider the extreme scenario of  $\theta = \pi/4$  and 300 scatterings (limited by our computational power). Even in this case the symmetric bound state is hardly affected and thus stable for all practical purposes near  $K = 0$ , see Supplements.

*Conclusion*— We have shown that bound states made of photon-emitter polaritons act like truly composite particles when tunneling between waveguides or generally being transformed in beamsplitter-like fashion. Two photons of a bound state cannot tunnel individually between waveguides and especially for  $\theta \ll 1$  this results in a trapping of the bound state over periods of time where free polaritons would have already completely switched modes. Additionally, we identified the emergence of new bound state configurations in the setup of two close-by

waveguides coupled to two-level emitters. Due to varying group velocities the different species of bound states can be spatially separated from each other as well as from the free polaritons. The Hong-Ou-Mandel effect at  $\theta = \pi/4$ , i.e. a 50/50 beamsplitter transformation between each pair of emitters, even allows for bound states with persistent self-oscillations. On a conceptual level, our results demonstrate that photon bound states show characteristics one would intuitively expect from a rigid molecule formed by photons. In the still mostly unexplored field of photons acting like bound matter, this promises for even more interesting phenomena, e.g. bound states interacting among themselves or being manipulated externally.

*Acknowledgements*— B.S. is supported by Deutsche Forschungsgemeinschaft (DFG, German Research Foundation), Grant No. 449674892. We acknowledge the support of Danmarks Grundforskningsfond (DNRF 139, HyQ Center for Hybrid Quantum Networks).

- 
- [1] D. E. Chang, V. Vuletić, and M. D. Lukin, Quantum nonlinear optics—photon by photon, *Nature Photonics* **8**, 685 (2014).
- [2] J.-T. Shen and S. Fan, Strongly correlated two-photon transport in a one-dimensional waveguide coupled to a two-level system, *Physical review letters* **98**, 153003 (2007).
- [3] J.-T. Shen and S. Fan, Strongly correlated multiparticle transport in one dimension through a quantum impurity, *Physical Review A* **76**, 062709 (2007).
- [4] O. Firstenberg, T. Peyronel, Q.-Y. Liang, A. V. Gorshkov, M. D. Lukin, and V. Vuletić, Attractive photons in a quantum nonlinear medium, *Nature* **502**, 71 (2013).
- [5] Q.-Y. Liang, A. V. Venkatramani, S. H. Cantu, T. L. Nicholson, M. J. Gullans, A. V. Gorshkov, J. D. Thompson, C. Chin, M. D. Lukin, and V. Vuletić, Observation of three-photon bound states in a quantum nonlinear medium, *Science* **359**, 783 (2018).
- [6] B. Bakkensen, Y.-X. Zhang, J. Bjerlin, and A. S. Sørensen, Photonic bound states and scattering resonances in waveguide qed, arXiv preprint arXiv:2110.06093 (2021).
- [7] G. Calajó and D. E. Chang, Emergence of solitons from many-body photon bound states in quantum nonlinear media, *Physical Review Research* **4**, 023026 (2022).
- [8] O. A. Iversen and T. Pohl, Strongly correlated states of light and repulsive photons in chiral chains of three-level quantum emitters, *Physical Review Letters* **126**, 083605 (2021).
- [9] Y. Ke, A. V. Poshakinskiy, C. Lee, Y. S. Kivshar, and A. N. Poddubny, Inelastic scattering of photon pairs in qubit arrays with subradiant states, *Physical review letters* **123**, 253601 (2019).
- [10] B. Schriński and A. S. Sørensen, Polariton dynamics in one-dimensional arrays of atoms coupled to waveguides, *New Journal of Physics* **24**, 123023 (2022).
- [11] A. S. Sheremet, M. I. Petrov, I. V. Iorsh, A. V. Poshakinskiy, and A. N. Poddubny, Waveguide quantum electrodynamics: collective radiance and photon-photon correlations, *Reviews of Modern Physics* **95**, 015002 (2023).
- [12] M. J. Hartmann and M. B. Plenio, Strong photon nonlinearities and photonic mott insulators, *Physical review letters* **99**, 103601 (2007).
- [13] D. Chang, V. Gritsev, G. Morigi, V. Vuletić, M. Lukin, and E. Demler, Crystallization of strongly interacting photons in a nonlinear optical fibre, *Nature physics* **4**, 884 (2008).
- [14] M. Kiffner and M. J. Hartmann, Dissipation-induced tonks-girardeau gas of polaritons, *Physical Review A* **81**, 021806 (2010).
- [15] M. Kiffner and M. J. Hartmann, Dissipation-induced correlations in one-dimensional bosonic systems, *New Journal of Physics* **13**, 053027 (2011).
- [16] M. Hafezi, M. D. Lukin, and J. M. Taylor, Non-equilibrium fractional quantum hall state of light, *New Journal of Physics* **15**, 063001 (2013).
- [17] E. Kapit, M. Hafezi, and S. H. Simon, Induced self-stabilization in fractional quantum hall states of light, *Physical Review X* **4**, 031039 (2014).
- [18] A. Albrecht, L. Henriët, A. Asenjo-Garcia, P. B. Dieterle, O. Painter, and D. E. Chang, Subradiant states of quantum bits coupled to a one-dimensional waveguide, *New Journal of Physics* **21**, 025003 (2019).
- [19] Y.-X. Zhang and K. Mølmer, Theory of subradiant states of a one-dimensional two-level atom chain, *Physical Review Letters* **122**, 203605 (2019).
- [20] Y.-X. Zhang and K. Mølmer, Free-fermion multiply excited eigenstates and their experimental signatures in 1d arrays of two-level atoms, *Physical Review Letters* **128**, 093602 (2022).
- [21] D. J. Brod and J. Combes, Passive cphase gate via cross-kerr nonlinearities, *Physical Review Letters* **117**, 080502 (2016).
- [22] D. J. Brod, J. Combes, and J. Gea-Banacloche, Two photons co-and counterpropagating through n cross-kerr sites, *Physical Review A* **94**, 023833 (2016).
- [23] B. Schriński, M. Lamaison, and A. S. Sørensen, Passive quantum phase gate for photons based on three level

- emitters, *Physical Review Letters* **129**, 130502 (2022).
- [24] H. Shapourian and A. Shabani, Modular architectures to deterministically generate graph states, *Quantum* **7**, 935 (2023).
- [25] Y. Lai and H. Haus, Quantum theory of solitons in optical fibers. i. time-dependent hartree approximation, *Physical review A* **40**, 844 (1989).
- [26] Y. Lai and H. Haus, Quantum theory of solitons in optical fibers. ii. exact solution, *Physical Review A* **40**, 854 (1989).
- [27] S. Mahmoodian, G. Calajó, D. E. Chang, K. Hammerer, and A. S. Sørensen, Dynamics of many-body photon bound states in chiral waveguide qed, *Physical Review X* **10**, 031011 (2020).
- [28] V. Yudson, Dynamics of integrable quantum systems, *Zh. Eksp. Teor. Fiz* **88**, 1757 (1985).
- [29] Y.-X. Zhang, C. Yu, and K. Mølmer, Subradiant bound dimer excited states of emitter chains coupled to a one dimensional waveguide, *Physical Review Research* **2**, 013173 (2020).
- [30] M. Kiffner, W. Li, and D. Jaksch, Three-body bound states in dipole-dipole interacting rydberg atoms, *Physical review letters* **111**, 233003 (2013).
- [31] P. Bienias, S. Choi, O. Firstenberg, M. F. Maghrebi, M. Gullans, M. D. Lukin, A. V. Gorshkov, and H. Büchler, Scattering resonances and bound states for strongly interacting rydberg polaritons, *Physical Review A* **90**, 053804 (2014).
- [32] F. Letscher and D. Petrosyan, Mobile bound states of rydberg excitations in a lattice, *Physical Review A* **97**, 043415 (2018).
- [33] N. Tomm, S. Mahmoodian, N. O. Antoniadis, R. Schott, S. R. Valentin, A. D. Wieck, A. Ludwig, A. Javadi, and R. J. Warburton, Photon bound state dynamics from a single artificial atom, *Nature Physics* , 1 (2023).
- [34] P. Lodahl, S. Mahmoodian, S. Stobbe, A. Rauschenbeutel, P. Schneeweiss, J. Volz, H. Pichler, and P. Zoller, Chiral quantum optics, *Nature* **541**, 473 (2017).
- [35] N. V. Hauff, H. Le Jeannic, P. Lodahl, S. Hughes, and N. Rotenberg, Chiral quantum optics in broken-symmetry and topological photonic crystal waveguides, *Physical Review Research* **4**, 023082 (2022).
- [36] I. Söllner, S. Mahmoodian, S. L. Hansen, L. Midolo, A. Javadi, G. Kiršanskė, T. Pregolato, H. El-Ella, E. H. Lee, J. D. Song, *et al.*, Deterministic photon–emitter coupling in chiral photonic circuits, *Nature nanotechnology* **10**, 775 (2015).
- [37] B. Le Feber, N. Rotenberg, and L. Kuipers, Nanophotonic control of circular dipole emission, *Nature communications* **6**, 1 (2015).
- [38] S. Barik, A. Karasahin, S. Mittal, E. Waks, and M. Hafezi, Chiral quantum optics using a topological resonator, *Physical Review B* **101**, 205303 (2020).
- [39] T. Ramos, H. Pichler, A. J. Daley, and P. Zoller, Quantum spin dimers from chiral dissipation in cold-atom chains, *Physical review letters* **113**, 237203 (2014).
- [40] I. M. Mirza and J. C. Schotland, Multiqubit entanglement in bidirectional-chiral-waveguide qed, *Physical Review A* **94**, 012302 (2016).
- [41] E. Sánchez-Burillo, C. Wan, D. Zueco, and A. González-Tudela, Chiral quantum optics in photonic sawtooth lattices, *Physical Review Research* **2**, 023003 (2020).
- [42] S. Lorenzo, S. Longhi, A. Cabot, R. Zambrini, and G. L. Giorgi, Intermittent decoherence blockade in a chiral ring environment, *Scientific Reports* **11**, 12834 (2021).
- [43] O. A. Iversen and T. Pohl, Self-ordering of individual photons in waveguide qed and rydberg-atom arrays, *Physical Review Research* **4**, 023002 (2022).

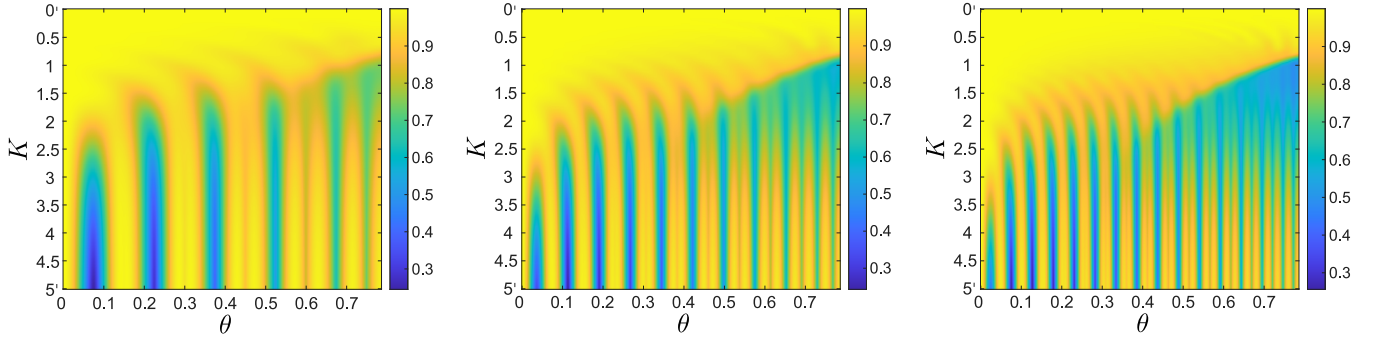


Figure 5. We study the stability of the symmetric bound state for  $K \neq 0$  for different number of scatterings  $N = 10$ ,  $N = 20$  and  $N = 30$  (left to right). The measure of stability is taken as the overlap with the exact eigenstate at  $K = 0$  (10). We observe a corridor of stability at  $K \simeq 0$ .

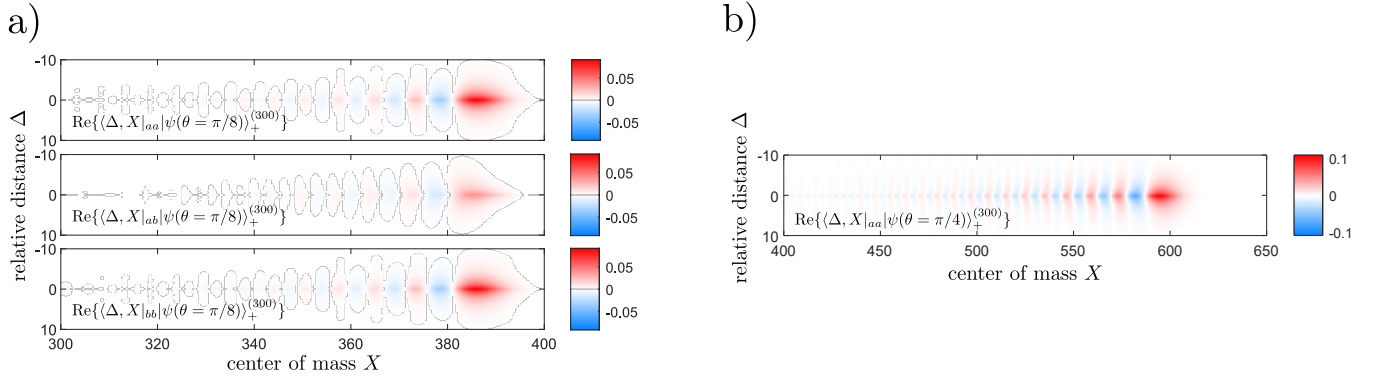


Figure 6. Wavefunction of the symmetric bound state at  $\theta = \pi/8$  and  $\theta = \pi/4$  after 300 scattering events. Because of the Hong-Ou-Mandel effect, in the latter case the state is zero in the  $ab$  mode after the 300th scattering and the respective wave function is not shown.

## Photon bound states: Supplemental material

In the main text we discuss the two newly emerging classes of bound states for coupled waveguides. While we can analytically show the stability of the anti-symmetric eigenstate, we can only describe the symmetric combination analytically for the special case of  $K = 0$ . A broad numerical study suggests that for  $K$  not close to 0 the symmetric state indeed decays, see Fig. 5. For this numerical study we calculate the overlap after 10, 20, 30 scatterings with the perfectly stable symmetric eigenstate (10) at  $K = 0$  for different tunneling strengths  $\theta$  and center-of-mass momentum  $K$ . We observe that there is a broad region of stability for small  $K$  that drops off sharply at large enough  $K$ .

This renders an input state tailored to maximize the bound state amplitude, e.g. a Gaussian with width  $\sigma_k = \Gamma/3$ , perfectly stable for all practical purposes. We show this exemplary for  $\theta = \pi/8, \pi/4$  and 300 scattering events in Fig. 6. Apart from ever present dispersion, the symmetric input state retains its bound state nature. We note that this numerical study is not a proof of instability beyond certain  $K$  as there is a possibility of more complex eigenstate different from (10) at finite  $K$ . Nevertheless, our findings do suggest that Eq. (10) is an excellent approximation for a stable eigenstate at  $K \simeq 0$ .

For completeness we also verify the  $e^{-\Gamma|\Delta|/2}$  decay expected for bound states for both the symmetric and anti-symmetric input state, see Fig. 7. Again inserting a Gaussian with  $\sigma_k = \Gamma/3$  there is no real quantitative difference between the symmetric and anti-symmetric input state apart from oscillating corrections due to the unbound portion.

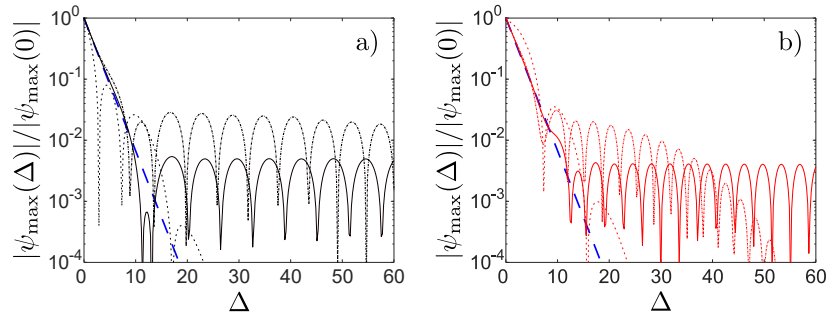


Figure 7. (a) Absolute value  $|\psi_{\max}(\Delta)|$  of the real space wave function of the symmetric bound state at  $\theta = \pi/4$ , maximized over the center of mass coordinate  $X$ . The different curves depict the state after 3 (dotted lines), 30 (dashed-dotted lines), and 300 (solid lines) scatterings, all normalized to the maximum value. The dashed curve marks the ideal  $e^{-\Gamma|\Delta|/2}$  decay of the bound state (1). (b) Same as in (a) but for the anti-symmetric bound state as reference.